Environmental Science and Pollution Research (2020) 27:37718–37732
https://doi.org/10.1007/s11356-020-09834-6

RESEARCH ARTICLE

Effects of acidic attack on chemical, mineralogical, and morphological properties of geomaterials

Suéllen Tonatto Ferrazzo[1] · Rafael de Souza Tímbola[2] · Lucimara Bragagnolo[1] · Elvis Prestes[3] · Eduardo Pavan Korf[1] · Pedro Domingos Marques Prietto[2] · Carina Ulsen[4]

Received: 11 January 2020 / Accepted: 22 June 2020 / Published online: 30 June 2020

Abstract

Exposure of geomaterials to acidic leachates may compromise their structure and functionality due to changes in physicochemical, mineralogical, and hydraulic behavior. The literature identifies the need to evaluate changes in a pure state and in conditions of extreme acidity. This study aimed to evaluate changes in the chemical, mineralogical, and morphological properties of Osorio fine uniform sand (OFS), basalt residual soil (BRS), kaolin (KAO), and bentonite (BEN) exposed to sulfuric acid in concentrations of 0.00 mol/L (distilled water), 0.01 mol/L, and 1.00 mol/L. The tested samples were characterized using X-ray fluorescence spectrometry, X-ray diffraction, thermogravimetry, differential scanning calorimetry, and scanning electron microscopy. The acid attack on geomaterials by contact with the solution 1.00 mol/L has resulted in the solubilization of some constituent minerals, as well as the formation of sulfate minerals, changes in the water dehydration peak in the pores, and mass loss. The morphology of the sand and bentonite particles did not change with exposure to sulfuric acid. The acidic attack resulted in changes in the morphology of the particles for BRS and KAO. The results of this study are important for determining operational parameters of waste containment systems and contaminated areas, as well as for applying geomaterials as founding materials.

Keywords Acidic leachate · Sulfuric acid · Sand · Basalt residual soil · Bentonite and kaolin · Chemical composition · Mineralogy and morphology

Responsible Editor: Philippe Garrigues

✉ Suéllen Tonatto Ferrazzo
suellenferrazzo@hotmail.com

Rafael de Souza Tímbola
rafaeltimbola@hotmail.com

Lucimara Bragagnolo
lucimarabragagnolo@hotmail.com

Elvis Prestes
prestes.elvis@gmail.com

Eduardo Pavan Korf
eduardo.korf@uffs.edu.br

Pedro Domingos Marques Prietto
pdmp@upf.br

Carina Ulsen
carina.ulsen@usp.br

[1] Graduate Program in Environmental Science and Technology, Federal University of Fronteira Sul, ERS 135, km 72, no 200, Erechim, RS 99700-970, Brazil

[2] Graduate Program in Civil and Environmental Engineering, University of Passo Fundo, BR 285, km 292, Passo Fundo, RS 99052-900, Brazil

[3] Federal University of Fronteira Sul, ERS 135, km 72, no 200, Erechim, RS 99700-970, Brazil

[4] Technological Characterization Laboratory, Department of Engenharia de Minas e Petróleo, University of São Paulo, Prof. Mello Moraes Avenue, 05508-030, Butantã, São Paulo, SP, Brazil

Introduction

Percolation of chemically aggressive liquids, like acidic waters from the leaching of industrial and mining wastes, may affect soil hydraulic behavior as a result of structure changes due to particle flocculation and reduced reactiveness. Over time, this outcome might compromise the functionality of geotechnical materials in waste containment systems leading to soil and groundwater contamination (Agbenyeku et al. 2016; Daniel et al. 1988; Hueckel et al. 1997; Knop et al. 2008). Furthermore, acid contamination of foundation soils can cause damage to industrial structures (structures of factory and industrial buildings) (Chavali et al. 2018).

In geoenvironmental and geotechnical applications, such as waste containment systems and remediation of contaminated areas, mixtures of clayey and cement, with or without bentonite, have been used to improve liners' hydraulic and reactive properties (Ghadr and Assadi-Langroudi2018; Gueddouda et al. 2016; Miguel et al. 2017; Morandini and Leite 2015; Wang et al. 2018). These soils also used in foundations may be contaminated with acids from natural or anthropogenic processes (Chavali et al. 2018). Therefore, it is of paramount importance to understand the behavior of such materials when exposed to aggressive conditions, in contact with inorganic acids (Chavali et al. 2017, 2018; Verástegui-Flores and Di Emidio 2014).

According to Chavali et al. (2018), several studies observed changes in the properties of soil contaminated by inorganic acid solutions (such as sulfuric acid) with a pH ranging from 3 to 6, which corresponds to natural conditions. The authors emphasized the need for studying the response of soil contaminated under more aggressive acidic conditions (pH lesser than 1), such as soil from acidic leachate storage ponds (Liu et al. 2013). In nature, the acidity of wastewater is derived from sulfuric acid molecules generated by the oxidation of sulfide minerals (for example, pyrite) in the presence of oxygen and water; this process is associated with acid mine drainage that has low pH values (in the range 0.8–4) (Knop et al. 2008). The pH is thus reduced by the presence of the acid, which increases the solubility of the soil and rock constituents. Soil contamination by sulfuric acid can be caused by anthropogenic processes, such as spills, leaks (Chavali et al. 2018), the use of sulfate scrubbers (or other minerals) in coal plants (Liu et al. 2013), or acid mine drainage (Agbenyeku et al. 2016; Buzatu et al. 2016; Miguel et al. 2017; Šucha et al. 2002).

Several studies have evaluated the effects of the exposure of geotechnical materials to different chemically aggressive solutions (Agbenyeku et al. 2016; Chavali et al. 2018; Hamdi and Srasra 2013; Li et al. 2013; Miguel et al. 2017; Šucha et al. 2002; Verástegui-Flores and Di Emidio 2014). These studies show that contact with acid water can cause mineralogical and physical–chemical changes in the properties of soil due to interactions with reactive components (Šucha et al. 2002), the reduced pH of the medium (Agbenyeku et al. 2016; Gratchev and Towhata 2013; Miguel et al. 2017), the dissolution of metals, the desorption of chemical species (Agbenyeku et al. 2016; Miguel et al. 2017), and cation exchange reactions with the partial dissolution of minerals (Chavali et al. 2018). The percolation of substances with high acidity can cause changes in the hydraulic conductivity of containment barriers consisting of clayey materials (Hamdi and Srasra 2013; Li et al. 2013; Liu et al. 2015).

In the study by Šucha et al. (2002), the acidification of the dystric cambisol by acid mine drainage resulted in the formation of jarosite and of amorphous and/or lower crystalline materials, rich in Si, Al, and Fe (mainly ferrihydrite). Miguel et al. (2017) conducted leaching tests on a tropical soil using acid mine drainage collected in a storage pond of uranium mining. The authors identified that effluents with pH lower than 6 promoted the formation of soil insoluble to the Al-F complexes and Fe, as well as Mg desorption above the specification of the Brazilian legislation. They also observed that the soil pH value decreases abruptly until the 6th month of acid percolation, and then slowly decreases, reaching 3.3 in the 12th month. According to Chavali et al. (2018), mineralogical change due to cation exchange and partial dissolution reactions reduces the swelling behavior of montmorillonite soils. The swelling behavior of three bentonites was evaluated by flooding soil under 1 N and 4 N sulfuric acid concentrations (98%) and quantified until expansion ceased (approximately 100 h). Acidified bentonites showed formation of sulfate-based minerals such as gypsum, halotrichite, potash alums, soda alums, tamaruchite, and melanterite. Regarding microstructure, the interaction with acid resulted in flocculation of soil particles. The contamination of sodium bentonite by H_2SO_4 caused a reduction in the expansion of this clay (116%), where equilibrium expandability of 67% and 50% was detected as the acid concentration increased. These changes in bentonite are due to the cation exchange process, in which sodium ion is replaced by hydrogen ion, whose ionic radius (0.012) is lower than that of sodium (1.02), resulting therefore in smaller expansions. However, there is still the need to know how the chemical, mineralogical, and morphological composition of geotechnical materials in pure state can be affected by contact with contaminants on pH below 1.

To that end, this work describes the changes in the chemical, mineralogical, and morphological properties of OFS, BRS, KAO, and BEN that have been exposed to sulfuric acid solutions. Understanding the effects of exposure to sulfuric acid solutions with low pH values on the properties of geomaterials is important in determining the operational parameters in geoenvironmental and geotechnical applications, such as in situ waste containment, the insulation of contaminated areas, and the use of geomaterials as founding materials. It is also

important to understand the extraction processes for chemical elements and metals present in these materials.

Materials and methods

Materials

The materials are OFS, BRS, KAO, BEN, and sulfuric acid. The sand was collected from a deposit in Osorio, state of Rio Grande do Sul (RS), Brazil. The clay soil used is BRS that was collected from the experimental field at the Geotecnia Ambiental do Centro Tecnológico (CETEC), University of Passo Fundo (UPF), Passo Fundo, RS, Brazil. KAO was purchased from a supplier of mineral products located in Pântano Grande, RS, Brazil. The white sodium BEN was obtained from a supplier at Soledade, state of Paraíba (PB), Brazil. The materials' description is shown in Table 1.

Methods

Material samples were air-dried and then oven-dried until 105 °C with hygroscopic moisture (3% to 5%). The samples were subsequently passed through a 2.0-mm sieve, according to NBR 6457 (ABNT 2016). The acidic attack on the material was studied by batch tests adapted from Standard D4646-03(ASTM 2008). The following variables were considered: sulfuric acid concentration at 0.00 mol/L, 0.01 mol/L, and 1.00 mol/L and four geomaterials (OFS, BRS, KAO, and BEN), resulting in 12 experiments.

The experiments consisted of inserting the samples of each material into an Erlenmeyer of 2000 mL, in proportion of 1 part of the soil to 20 of solution (ASTM 2008). They were kept immersed in the sulfuric acid solution and underwent continuous horizontal stirring for 24 h under 215 rpm and 22 ± 5 °C. In the end of the shaking process, the samples were decanted and centrifuged to separate the solid and liquid phases. The centrifugation process was performed in a centrifuge at 3000 rpm for 10 min (USEPA 1996). The resulting solid material was placed in porcelain capsules and oven-dried under constant temperature of 40–50 °C until mass constancy. The dried samples were placed in porcelain crucibles and macerated and conditioned in plastic bag, sealed, and identified for further analyses.

The geomaterial characterization and the evaluation of the changes in the particle properties were determined using X-ray fluorescence spectrometry (XRF), X-ray diffraction (XRD), thermogravimetry with differential scanning calorimetry (TG/DSC), and scanning electron microscopy (SEM). The chemical composition was determined using the XRF technical, in a pressed sample, using STD-1 calibration (standardless) for non-standard analysis of the chemical elements between fluorine and uranium, in a fluorescence spectrometer of X-ray Bruker brand, S8 Tiger model.

The crystalline structure of the phases of the materials was analyzed by XRD (Bruker model D8 Endeavor) with a position-sensitive detector. The samples were scanned between two theta values of 2.5–70° with a step size of 0.02°. The X-ray tube was operated at 40 kV and 35 mA. The identification of the crystalline phases was done by comparing the sample diffractogram with the PDF2 database of the International Center for Diffraction Data (ICDD) in the X'Pert High Score software. To aid in the interpretation of the mineralogical and chemical analyses, TG/DSC was performed in TA Instruments® equipment, model SDT-Q600 V 20.9 Build 20 for thermal analysis in an inert or oxidizing atmosphere until a temperature of 1400 °C was reached. To study the surface topography of the particles, the samples were analyzed using SEM, Tescan brand equipment, model Vega 3. The following analytical conditions were used in the analyses: backscattered electrons (BSE) with magnification of 800, 3000, 10,000, and 6000 times (OFS, BRS, KAO, and BEN respectively), electron beam of voltage of 10 kV, and energy-dispersive detector (EDS) mode.

Results and discussion

Chemical and mineralogical changes

Based on the chemical composition of the geomaterials samples (Table 2) and the XRD analysis (Figs. 1, 2, 3, and 4), the

Table 1 Description of materials

Material	Description
OFS	Fine, clean sand of uniform granulometry (ASTM 1993; ABNT 1995)
BRS	Oxisoil humic (Streck et al. 2008); low- to high-liquidity clay (ASTM 1993)
KAO	Low-plasticity inorganic silt (ASTM 1993)
BEN	Inorganic clay of high plasticity (ASTM 1993)
Sulfuric acid	P.A., Merck brand with purity 95–97% and density 1.84 g/cm^3
	Sulfuric acid solutions: 0.00 mol/L (pH of distilled water equal to 7 ± 2), 0.01 mol/L (pH 2), and 1.00 mol/L (pH 0)

Table 2 Chemical composition (XRF) of the studied geomaterial samples (in percentage)

Sample	SiO_2	Al_2O_3	Fe_2O_3	K_2O	Na_2O	CaO	TiO_2	SO_3
OFS	93.1	2.20	0.40	0.86	0.12	0.06	0.15	0.02
OFS distilled water	95.3	1.87	0.30	0.73	0.12	0.05	0.11	0.00
OFS 0.01 mol/L	94.1	1.87	0.29	0.72	0.11	0.04	0.09	0.05
OFS 1.00 mol/L	85.9	1.10	0.28	0.62	0.00	0.00	0.08	2.82
BRS	46.4	24.2	10.70	0.40	0.00	0.04	1.64	0.07
BRS distilled water	49.7	20.7	10.50	0.37	0.00	0.04	1.57	0.07
BRS 0.01 mol/L	48.8	22.9	11.20	0.43	0.00	0.03	1.67	0.37
BRS 1.00 mol/L	20.1	7.09	3.86	0.14	0.00	0.03	0.64	15.9
KAO	47.4	35.8	1.17	0.84	0.00	0.11	0.15	0.08
KAO distilled water	46.4	36.2	1.66	1.07	0.00	0.12	0.22	0.00
KAO 0.01 mol/L	45.7	33.6	1.21	0.93	0.00	0.10	0.16	0.22
KAO 1.00 mol/L	30.7	24.3	0.89	0.67	0.00	0.10	0.10	7.93
BEN	46.5	31.4	2.62	1.24	0.80	1.17	0.36	0.03
BEN distilled water	52.9	24.6	2.25	2.90	0.33	2.49	0.26	0.00
BEN 0.01 mol/L	48.2	25.9	3.09	1.14	0.33	1.14	0.41	0.30
BEN 1.00 mol/L	34.7	19.4	1.85	0.22	0.12	0.22	0.25	8.88

presence of quartz in the OFS has been verified and also was corroborated by the high SiO_2 content (about 94%). The presence of kaolinite in BRS, KAO, and BEN has been also observed, confirmed by aluminum content of 24.2%, 35.8%, and 31.4%, respectively. The presence of hematite (10.7% F_2O_3 content) and quartz in the BRS, KAO, and BEN samples was identified. All geomaterials had increased SO_3 content due to their adsorption in the active sites of the materials. With the exception of OFS, the others had shown the formation of alunogen (sulfate mineral) in the samples exposed to the 1.00 mol/L acidic solution. Chavali et al. (2018) found that black cotton soil flooded for 100 h in 4 N sulfuric acid solution resulted in calcite dissolution, and formation of new alunogen and bassanite minerals. According to the authors, changes in the soil cation exchange complex and subsequent interactions of cations and anions led to the formation of new minerals.

As can be seen in Table 2, the geomaterial samples exposed to the acid attack showed significant loss of the main constituent oxides, but these losses were less significant in the OFS. The OFS exposed to the 1.00 mol/L solution showed a SiO_2 content of 85.9%, while the other samples had an average content of 94%, corresponding to a reduction of around 9%.

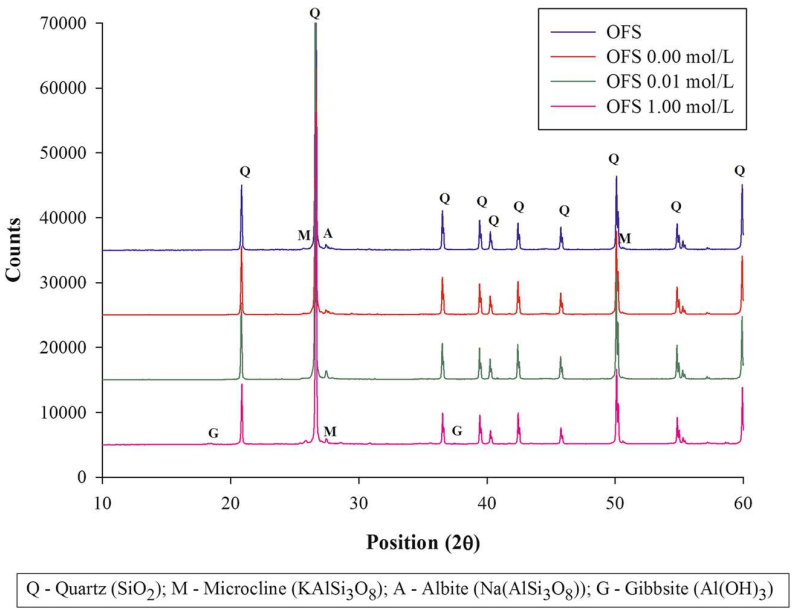

Fig. 1 XRD analysis of OFS samples

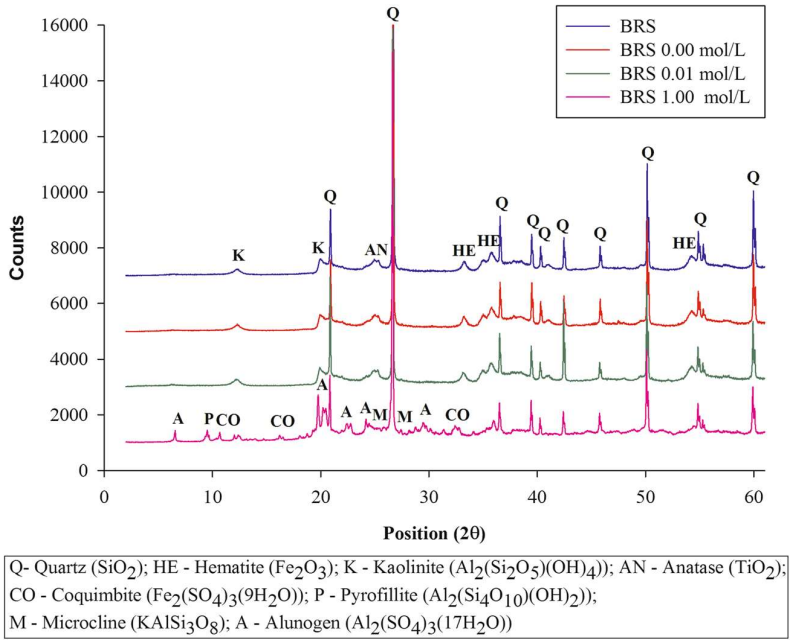

Fig. 2 XRD analysis of BRS samples

The OFS had the lowest reduction of SiO_2 because it mostly consists of quartz, and the sulfuric acid attacked the geomaterials' amorphous phase. This is in line with the findings of MacCarthy et al. (2014), who found that the dissolution rate of SiO_2 is not very significant and is lower than the observed rate for hematite in lateritic soil under pH of 1.

MacCarthy et al. (2014) state that the solubility range for quartz under 25 °C corresponds to the dissolution of amorphous silica. The authors also report that the presence of Fe, Al, Mg, Si, and Na in the minerals also affected the adsorption and the attack of the H^+ ions on the active sites of the quartz and hematite particles. In the quartz, the liberation of Si and Na occurred, with faster and preferential liberation of Na. In the hematite, the dissolution of Fe was followed by that of Al. In addition, there was a 56.7% loss of SiO_2 in the BRS, while in the OFS it was 7.7%. This is because in the pH 0

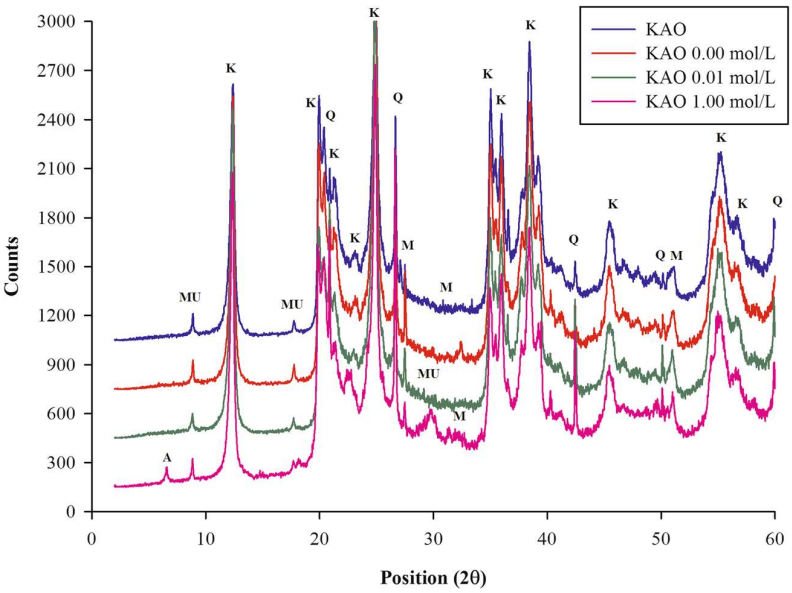

Fig. 3 XRD analysis of KAO samples

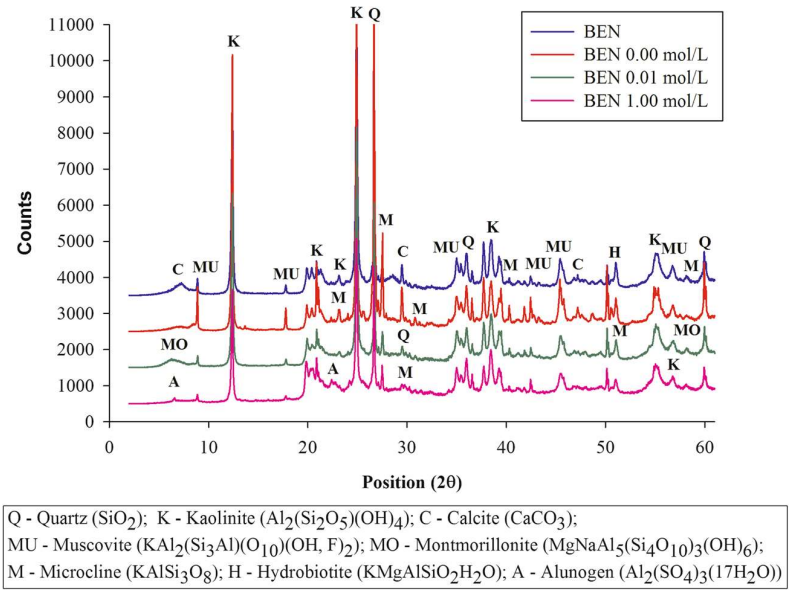

Fig. 4 XRD analysis of the BEN samples

solution the dissolution rate of silicates was controlled by other constituent oxides present in a higher concentration in the BRS than in the OFS, as OFS mostly consists of SiO_2(Brady and Walther 1989). This is because at high pH values the Si surface sites are deprotonated, and the control of the total dissolution rate of the silicate occurs by the displacement of the Si. The zero charge point for SiO_2(quartz) is at low pH values, around 2.4, and at 25 °C. This corresponds to the pH at which the surface charge is controlled by the other constituent oxides, in which case the release of non-constituent oxides of the silicon structure determines the rates of dissolution of multiple silicate oxides. In the samples of geomaterials 0.00 mol/L (distilled water) and 0.01 mol/L there was an increase in SiO_2 content in relation to the untested geomaterial; this difference is small and considered negligible, varying according to the representativeness of the sample.

It should be noted that in this study, the exposure of sandy, silty, and clayey geomaterials to the distilled water (pH~6.5) and the 0.01 mol/L (pH 2) sulfuric acid solution did not cause SiO_2 dissolution of the material structure. However, the contact with the pH 0 acidic solution resulted in a SiO_2 content reduction of 7.73% for OFS, 57.59% for BRS, 35.25% for KAO, and 25.38% for BEN. This case can be explained by the fact that, at extreme pH levels (< 2), the surface of the quartz mineral has the highest concentration of protonated sites, resulting in a higher rate of dissolution. In the pH range of 2 to 4, the neutral sites dominate and, as the dissolution of these sites is lower, the rate of dissolution is reduced. In the higher pH ranges, the number of deprotonated sites increases, resulting in a new rate increase (Nangia and Garrison 2010). The higher solubility observed for BRS, KAO, and BEN shows a loss related to the SiO_2 present in clayey minerals, according to the mineralogy described in Fig. 1.

Figure 1 shows the comparative diffractograms of pure OFS samples and of the samples exposed to sulfuric acid under different concentrations. It has been verified that there were little changes in the geomaterial composition, as approximately 94% of the sample is composed of quartz (Table 2) and this mineral is not very reactive to sulfuric acid. This is in line with the study by Knauss and Wolery (1988), wherein the evaluation of the dissolution kinetics of quartz under pH range of 1.4–11.8 at 70 °C demonstrated that the rate of dissolution of the mineral is more pronounced in pH 8. This is also in line with MacCarthy et al. (2014), who report the slow release of Si under pH 1 and 25 °C.

According to the XRF analysis, the OFS 1.00 mol/L sample had more significant chemical changes in the oxide content, thus corroborating the XRD data that revealed the albite dissolution and gibbsite formation, probably due to the exposure to the acidic pH 0 solution, and under agitation for 24 h promotes acceleration of the contact of soil particles with acid. These conditions correspond to an extreme environment that simulates long term. That solution and a temperature of 22 ± 5 °C were the conditions that resulted in the dissolution of the albite in the OFS, as it is reported that this process occurs under pH of 1–4 at a temperature of 25–90 °C (Rose 1991). Furthermore, the formation of gibbsite is probably due to the loss of silica from the structure of the material, as demonstrated by XRF analysis. According to Blight and Leong (2012), the gibbsite formation occurs as there is silica loss and presence of aluminum oxide in the free phase.

The XRD analysis of the BRS samples revealed that the main minerals in this soil are quartz (SiO_2), kaolinite, hematite, and anatase (Fig. 2). The presence of microclinic, alunogen, coquimbite, and pyrophyllite has been identified and the absence of hematite and anatase in the sample exposed

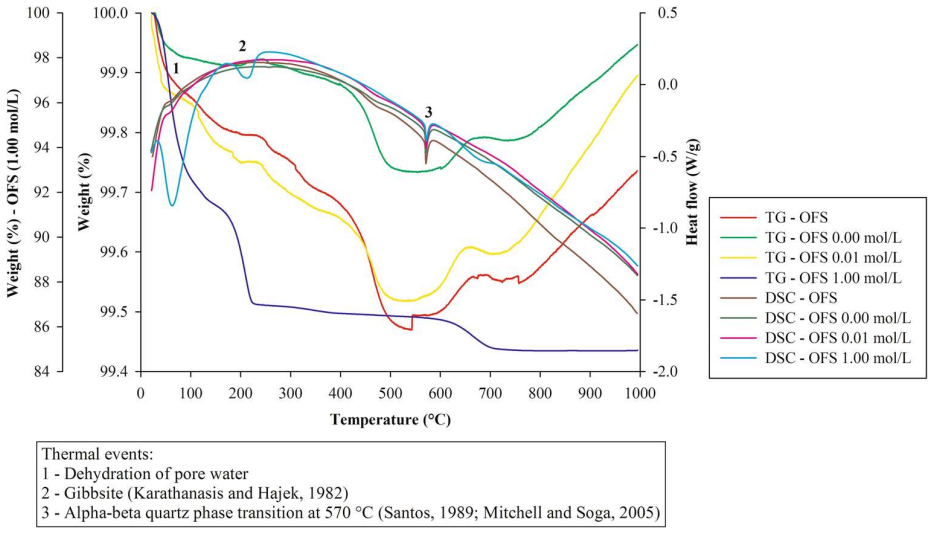

Fig. 5 TG and DSC analyses of OFS samples

to the extreme acid attack. The loss of these minerals in the BRS 1.00 mol/L (pH 0) sample occurred because the acidic attack caused more significant loss of Fe_2O_3 and TiO_2, according to XRF data. The alunogen, identified in the BRS 1.00 mol/L sample, corresponds to one of the hydrated sulfates formed through the acid weathering of aluminosilicates (Košek et al. 2018) and the aluminum precipitation in extreme acidity (Buzatu et al. 2016; Gil 2016; Hudson-Edwards et al. 1999). In the BRS 1.00 mol/L sample, the presence of iron sulfate, coquimbite, is an indication of high oxidation conditions. In other studies, this mineral was verified in acidic wastewater soils with pH less than 2 (Buckby et al. 2003; Gil 2016; Hudson-Edwards et al. 1999) and in areas affected by acid mining drainage (Buzatu et al. 2016). Šucha et al. (2002) reported the presence of pyrophyllite, also identified in the BRS 1.00 mol/L sample, in dystrophic cambisol with a mean pH of 2.3 that was strongly affected by acidic mining drainage.

The XRD analysis of the KAO samples (Fig. 3) confirmed there was little change in the composition of KAO before the acidic attack, compared to the other materials analyzed, because the crystalline phase of kaolin was not reached due to kaolinite being a mineral with low chemical reactivity. The geomaterial samples exposed to sulfuric acid changed significantly in terms of oxide content (Table 2) but retained the main constituent minerals. This is because KAO mainly consists of silicates the dissolution pH range of which does not include the values of this study (pH 2 and pH 0), as a large number of minerals in this class undergo dissolution under pH range of 5–12 at 25 °C (Brady and Walther 1989). The presence of alunogen has been also verified in the KAO 1.00 mol/L sample.

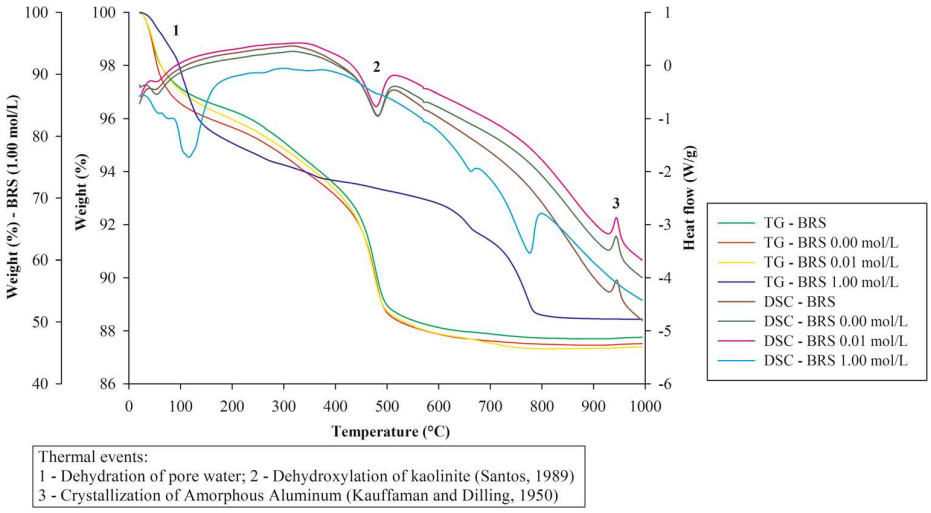

Fig. 6 TG and DSC analyses of BRS samples

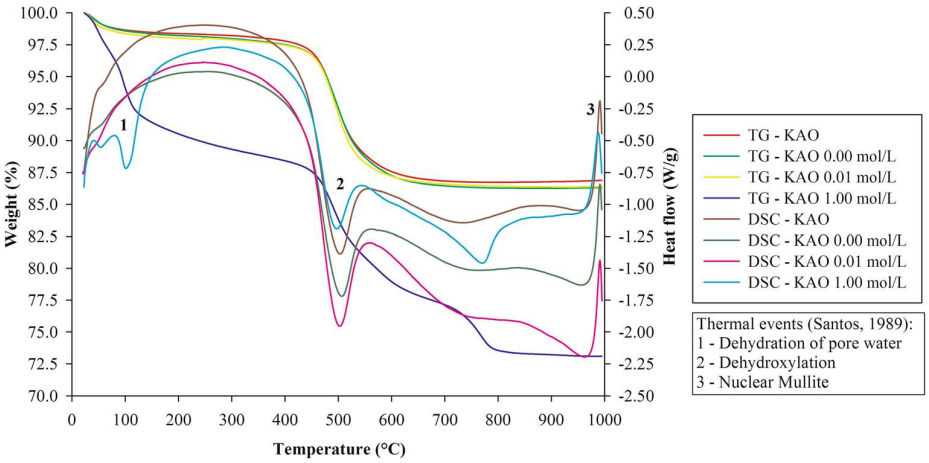

Fig. 7 TG and DSC analyses of KAO samples

The XRD results for the BEN samples (Fig. 4) show the presence of montmorillonite (BEN 0.01 mol/L) and alunogen (BEN 1.00 mol/L) and the calcite and hydrobiotite loss in both samples. The acidic attack may have caused the dissolution of the calcite in the BEN 0.01 mol/L and BEN 1.00 mol/L samples because the contaminant solutions had lower pH values (2 and 0, respectively), as the dissolution of this mineral by mass transfer was reported in regions of pH below 4 and 25 °C (Berner and Morse 1974; Morse and Arvidson 2002). Under these conditions, the dissolution rate is proportional to the concentration of H^+ ions, and it is independent, under pH higher than 5.5 (Sjoberg and Rickard 1984).

Figure 5 shows the TG and DSC results for the OFS samples and the observed thermal events. It has been verified that only the sample exposed to the most concentrated acid solution showed a significant mass in thermal event 1, characterized by dehydration of the pores. In the OFS 1.00 mol/L sample, event 2 is identified, which corresponds to the endothermic peak of gibbsite. This corroborates the XRD results in which gibbsite formation was observed. However, the acidic attack has not caused the change in the peak that characterizes polymorphic transformations of α-quartz to β-quartz (event 3). It has been observed that during the heating only the OFS 1.00 mol/L sample lost significant mass, equivalent to 15.06%. Most of this reduction occurred when the temperature reached 220 °C and hovered around 2% until the end of the analysis. This evidence confirms that the exposure under 1.00 mol/L sulfuric acid modifies the quartz resistance with respect to the dehydration of adsorbed water and is also related to the formation of the hydrated mineral gibbsite (Fig. 1), which may have contributed to the loss of mass of the OFS 1.00 mol/L sample. The other samples have shown mass gain in the end of the test resulting from secondary reactions in the heating chamber.

The TG and DSC results for the BRS samples (Fig. 6) show reductions in the thermal event values for BRS exposed to the

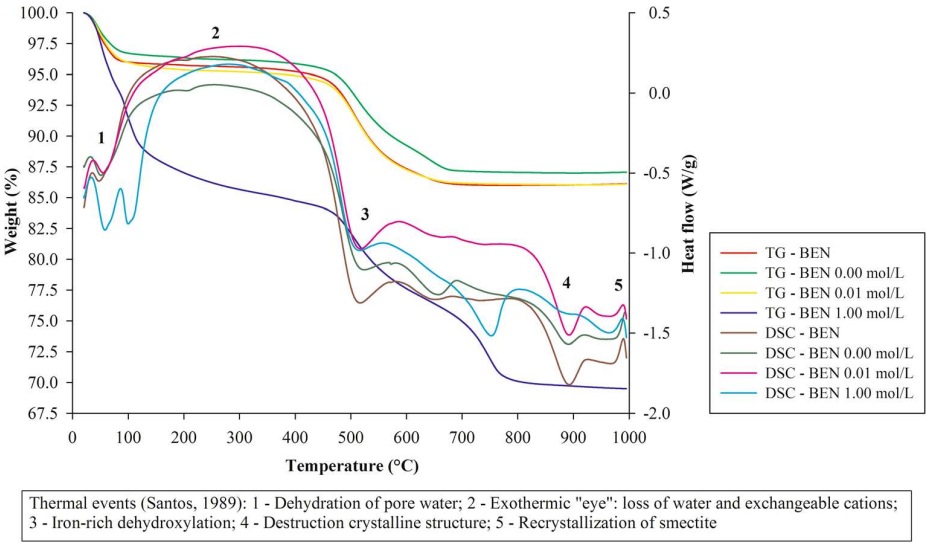

Fig. 8 TG and DSC analyses of BEN samples

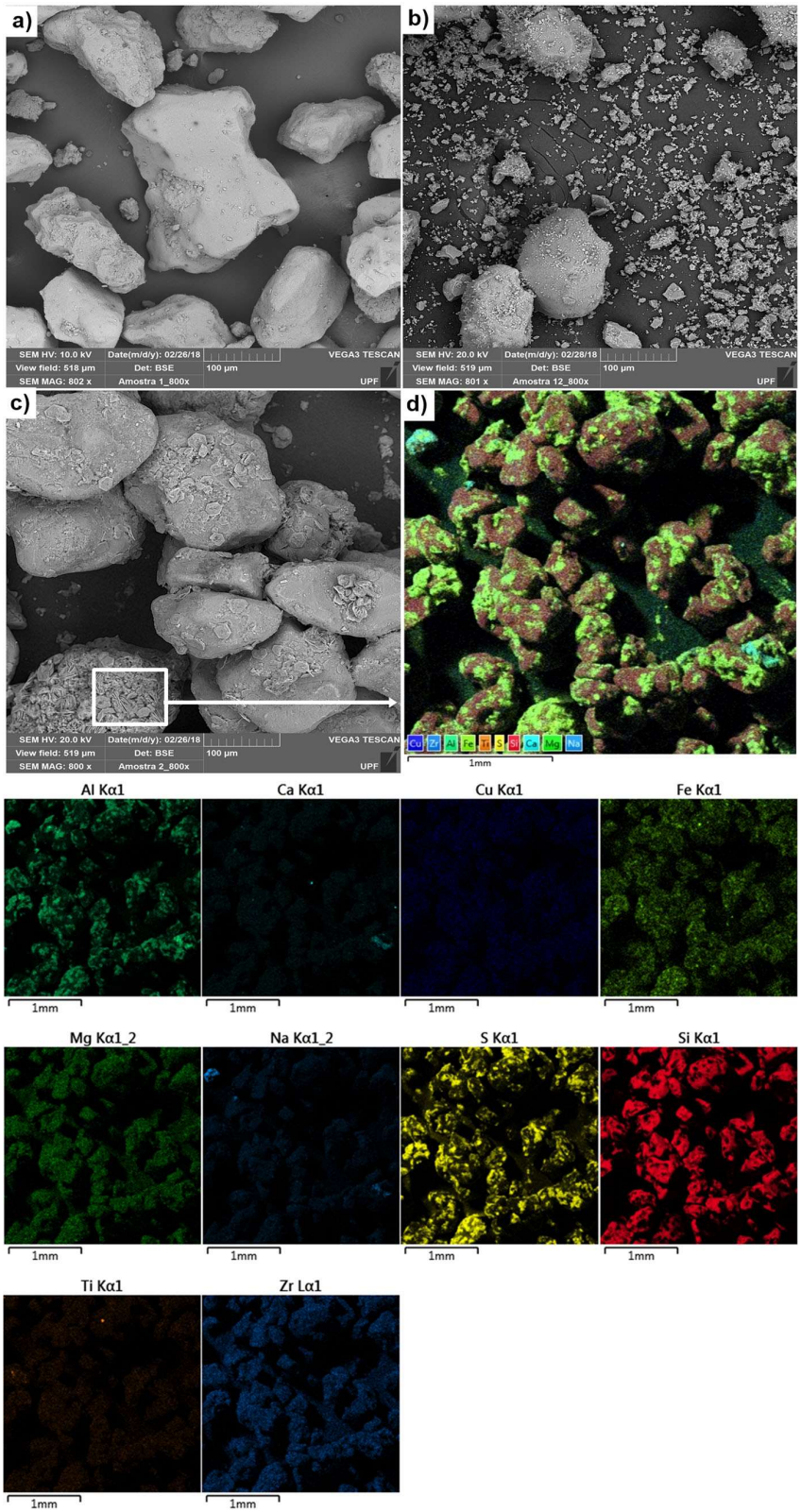

Fig. 9 Morphology of **a** the OFS particles, **b** the OFS 0.00 mol/L, and **c** the OFS 1.00 mol/L; **d** magnification with chemical map and distribution of the elements

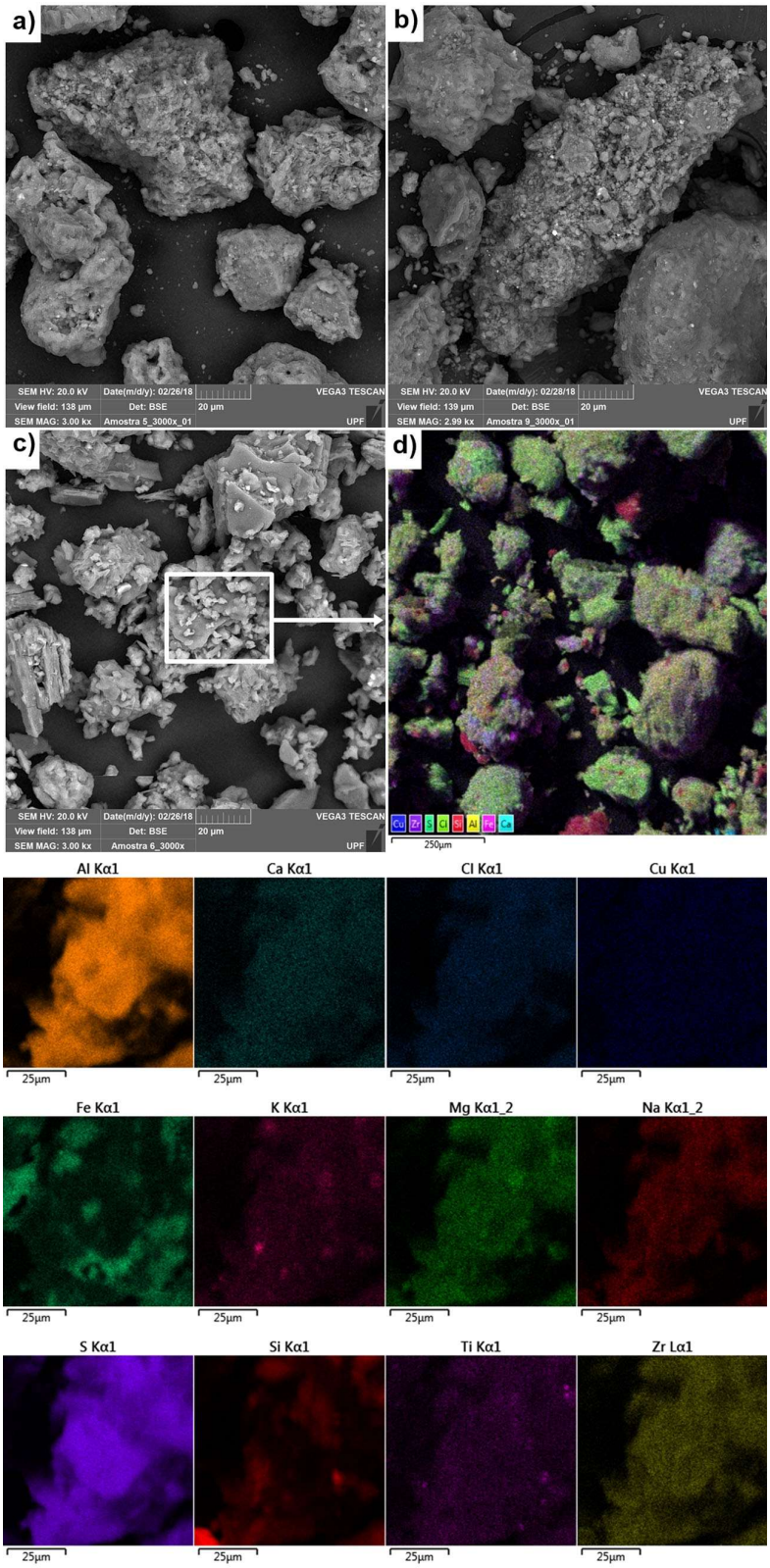

Fig. 10 Morphology of **a** the BRS particles, **b** the BRS 0.00 mol/L, and **c** the BRS 1.00 mol/L; **d** magnification with chemical map and distribution of the elements

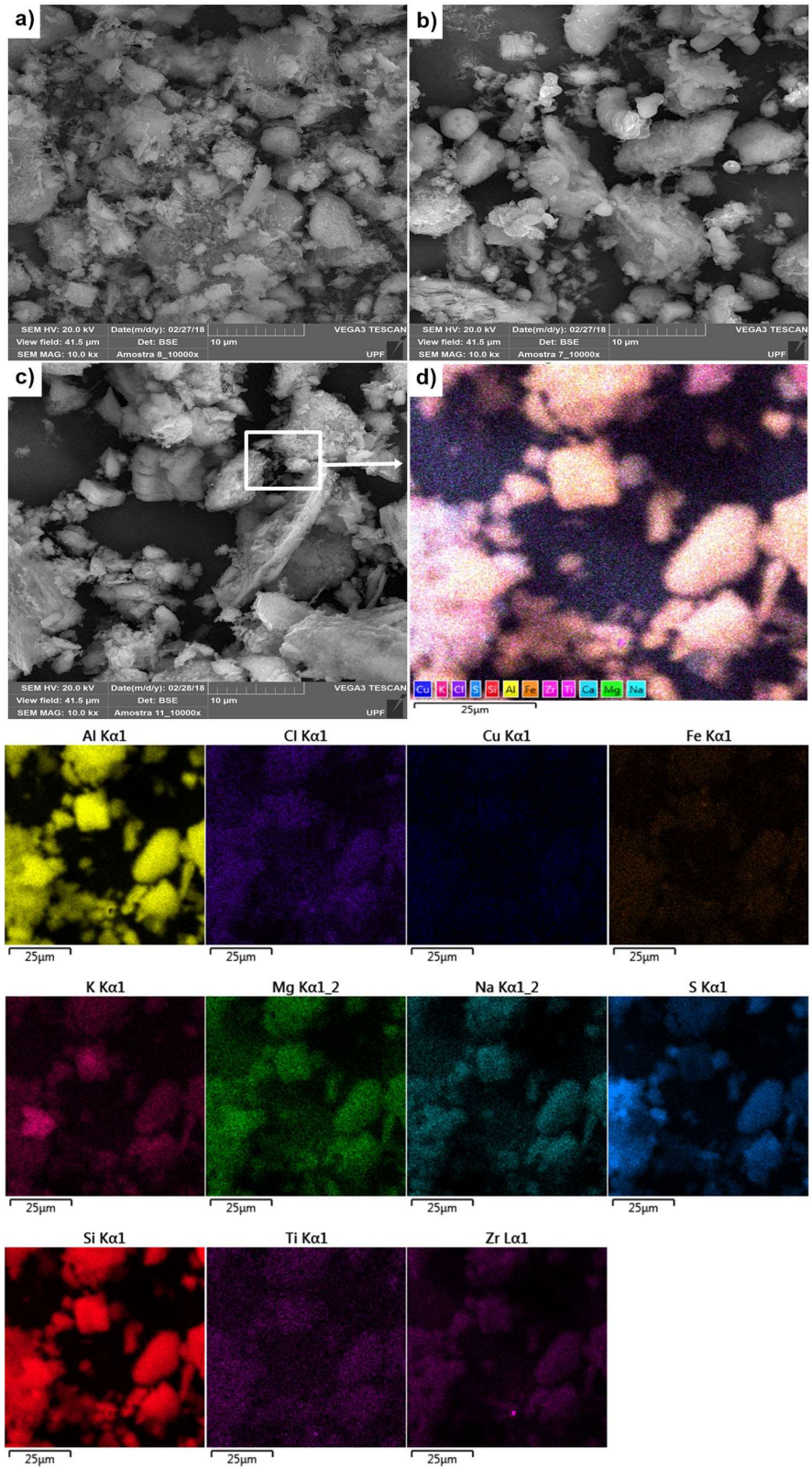

Fig. 11 Morphology of **a** the KAO particles, **b** the KAO 0.00 mol/L, and **c** the KAO 1.00 mol/L; **d** magnification with chemical map and distribution of the elements

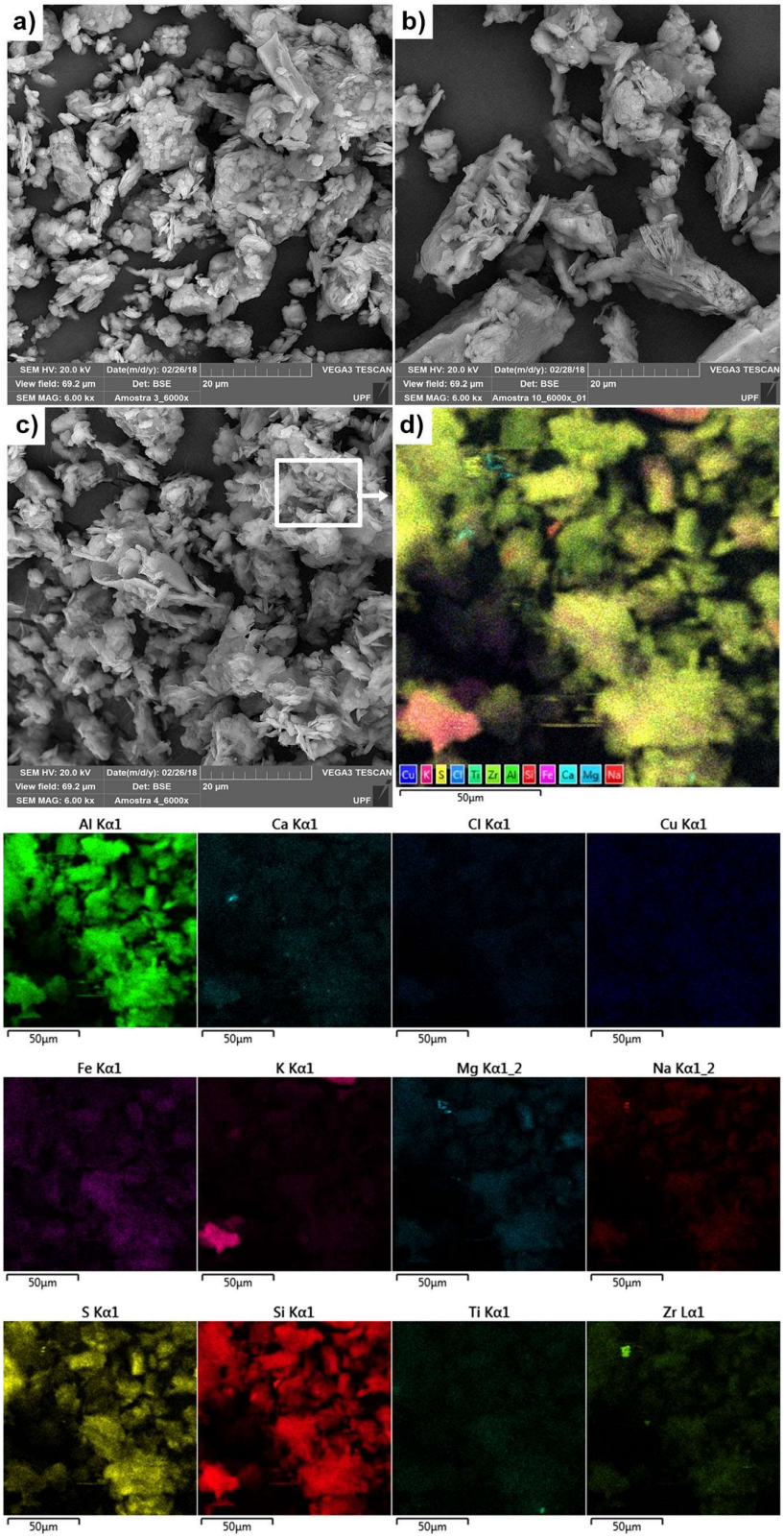

Fig. 12 Morphology of **a** the BEN particles, **b** the BEN 0.00 mol/L, and **c** the BEN 1.00 mol/L; **c** magnification with chemical map and distribution of the elements

1.00 mol/L acid solution. In this sample, the endothermic peak of dehydration of adsorbed water (event 1) occurred under a temperature of 114.65 °C and was observed at lower temperatures in the other samples. The transformation peak of kaolinite to metakaolinite (dehydroxylation) (event 2), which for kaolinitic soils should occur in the temperature range of 450 to 600 °C (Santos 1989), was identified in 774 °C in the BRS 1.00 mol/L sample. The reduction of the value of event 3 has been also observed, characterized by the exothermic peak of crystallization of the amorphous aluminum, in the BRS 1.00 mol/L sample. These changes may have occurred as a result of reactions between the soil and sulfuric acid compounds, the content reduction of the main constituent oxides, and the increase in the SO_3 concentration. This was confirmed by the formation of coquimbite and alunogen, according to the XRD results. The BRS 1.00 mol/L sample also showed the maximum mass loss, corresponding to 49.55%. This occurred because the acidic attack caused the formation of hydrated minerals and sulfates, such as pyrophyllite, coquimbite, and alunogen, identified by XRD (Fig. 2).

Figure 7 shows the TG and DSC results for the KAO samples and the identified thermal events. It can be seen that the sample exposed to the 1.00 mol/L acid solution showed a more significant mass loss in thermal event 1, which corresponds to dehydration of the pores. A mass loss of 26.93% has been verified for the KAO 1.00 mol/L sample, the maximum reduction among the samples. Another factor that may have contributed to this mass loss is the alunogen formation.

The TG and DSC analyses of the BEN samples are shown in Fig. 8, along with the major thermal events. In the other samples, the BEN exposed to the 1.00 mol/L sulfuric acid solution has shown changes in the peaks that characterize the loss of moisture/adsorbed water (event 1) and the loss of exchangeable cations (event 2), such as Ca^{2+} and Na^{+}. This is corroborated by the XRF data that has demonstrated the reduction of the CaO and Na_2O contents and the temperature modification that marks the destruction of the crystalline structure (event 4). Furthermore, the BEN 1.00 mol/L sample was the one that has suffered the largest loss of mass, 30.47%, which may also have occurred by the alunogen formation because it is a hydrated mineral ($Al_2(SO_4)_3(17H_2O)$) that contributed to the greater loss of water in the sample (Fig. 4).

Microstructure analysis

Figures 9, 10, 11, and 12 show SEM images of the pure geomaterials and those submitted to the acid solutions under range (distilled water and 1.00 mol/L). SEM analysis showed that the acidic attack does not seem to have caused changes in the particle morphology of the OFS samples (Fig. 9), which are relatively rounded and uniform, as described by Forcelini et al. (2016). It has been also possible to observe the heterogeneous arrangement of small particles of the sand particles subjected to the extreme sulfur attack (Fig. 9c, d) which perhaps were composed of sulfur and other products of acid attack reactions to the OFS (Fig. 9d).

BRS and KAO are small, stacked, squamous particles forming agglomerates (Figs. 10 and 11). Figure 10c, d shows the noticeable surface changes of the 1.00 mol/L BRS sample, and Fig. 10d shows the formation of chemical elements deposited on the particles. Figure 11b shows the deposition of a large amount of elements on the particles of the 0.01 mol/L KAO sample. The same was observed in the 1.00 mol/L KAO sample. The acidic attack resulted in more voids between the particles (Fig. 10c–d). The morphology of BEN, characterized by clusters of clay minerals and quartz that make up small dispersed particles in the sample (Fig. 12) and which has been preserved against exposure to the acidic contaminant, is similar to that of the clay in nearby municipalities, such as Cubati and Pedra Lavrada (PB)(Tonnesen et al. 2012), which has been preserved against exposure to the acidic contaminant.

Conclusions

This study described the changes in the chemical, mineralogical, and morphological properties of OFS, BRS, KAO, and BEN exposed to sulfuric acid solutions. Exposure to the 1.00 mol/L solution has caused significant reductions in the main constituent oxide content but a less significant reduction in the OFS and an increase in the SO_3 content.

The acidic attack under 1.00 mol/L also resulted in mineralogical changes in the geomaterials through partial dissolution of minerals and formation of new minerals, as well as greater loss of mass.

In the studied geomaterials, after exposure to the acid, no changes in the morphology of the OFS and BEN particles have been observed. However, the acidic attack resulted in changes in the BRS and KAO particles, with the formation of deposits of chemical elements and voids between the particles. Geomaterial chemical and mineralogical and effluent pH composition are key factors for higher or lower reactivity as acid contaminant.

The evidence described in this study demonstrates that the contact of geomaterials with sulfuric acid over time will negatively impact their structure and capacity to retain contaminants, or as foundation materials exposed to acidic wastewater. The information presented is relevant for determining the operating conditions for extracting compounds or metals of interest from geomaterials containing sand or silt.

Acknowledgments The authors wish to express their gratitude to FAPERGS (Process 16/2551-0000205-3, Programs First Projects - ARD/PPP/FAPERGS/CNPq) for financial support to the research group.

References

ABNT (1995) Rochas e Solos - NBR 6502. ABNT, Rio de Janeiro, BR, 18 p

ABNT (2016) Amostras de Solo: Preparação para Ensaios de Compactação e Ensaios de Caracterização - NBR 6457. ABNT, Rio de Janeiro, BR, 12 p

Agbenyeku EE, Muzenda EM, Msibi MI (2016) Chemical alterations in three clayey soils from percolation and interaction with acid mine drainage (AMD). S Afr J Chem Eng 21:28–36. https://doi.org/10.1016/j.sajce.2016.04.003

ASTM (1993) Standard practice for classification of soils for engineering purposes (unified soil classification system) - D2487–06. ASTM International, West Conshohocken, Pennsylvania, USA, 12 p

ASTM (2008) Standard test method for 24-h batch-type measurement of contaminant sorption by - D4646–03. ASTM International, West Conshohocken, Pennsylvania, USA, 4 p

Berner RA, Morse JW (1974) Dissolution kinetics of calcium carbonate in sea water; IV, theory of calcite dissolution. Am J Sci 274(2):108–134. https://doi.org/10.2475/ajs.274.2.108

Blight GE, Leong EC (2012) Mechanics of residual soils. In: Climate change 2013 - the physical science basis. CRC Press, New York. https://doi.org/10.1017/CBO9781107415324.004

Brady PV, Walther JV (1989) Controls on silicate dissolution rates in neutral and basic pH solutions at 25°C. Geochim Cosmochim Acta 53(11):2823–2830. https://doi.org/10.1016/0016-7037(89)90160-9

Buckby T, Black S, Coleman ML, Hodson ME (2003)Fe-sulphate-rich evaporative mineral precipitates from the Rio Tinto, Southwest Spain. Mineral Mag 67(2):263–278. https://doi.org/10.1180/0026461036720104

Buzatu A, Dill HG, Buzgar N, Damian G, Maftei AE, Apopei AI (2016) Efflorescent sulfates from Baia Sprie mining area (Romania)- acid mine drainage and climatological approach. Sci Total Environ 542:629–641. https://doi.org/10.1016/j.scitotenv.2015.10.139

Chavali RVP, Vindula SK, Reddy PHP, Babu A, Pillai RJ (2017) Swelling behavior of kaolinitic clays contaminated with alkali solutions: a micro-level study. Appl Clay Sci 135:575–582. https://doi.org/10.1016/j.clay.2016.10.045

Chavali RVP, Reddy HPP, Murthy RV, Sivapullaiah PV (2018) Swelling characteristics of soils subjected to acid contamination. Soils Found 58:110–121. https://doi.org/10.1016/j.sandf.2017.11.005

Daniel DE, Liljestrand HM, Broderick GP, Haven W, Bowders JJ (1988) Interaction of earthen liner materials with industrial waste leachate. Hazard Waste Hazard Mater 5(2):93–108. https://doi.org/10.1089/hwm.1988.5.93

Forcelini M, Garbin GR, Faro VP, Consoli NC (2016) Mechanical behavior of soil cement blends with Osorio sand. Proc Eng 143:75–81. https://doi.org/10.1016/j.proeng.2016.06.010

Ghadr S, Assadi-Langroudi A (2018)Structure-based hydro-mechanical properties of sand-bentonite composites. Eng Geol 235:53–63. https://doi.org/10.1016/j.enggeo.2018.02.002

Gil JAG (2016) Drenaje Ácido de Mina en la Faja Pirítica Ibérica: Técnicas de Estudio e Inventario de Explotaciones. Universidad de Huelva, Huelva

Gratchev I, Towhata I (2013)Stress-strain characteristics of two natural soils subjected to long-term acidic contamination. Soils Found 53(3):469–476. https://doi.org/10.1016/j.sandf.2013.04.008

Gueddouda MK, Goual I, Benabed B, Taibi S, Aboubekr N (2016) Hydraulic properties of dune sand–bentonite mixtures of insulation barriers for hazardous waste facilities. J Rock Mech Geotech Eng 8(4):541–550. https://doi.org/10.1016/j.jrmge.2016.02.003

Hamdi N, Srasra E (2013) Hydraulic conductivity study of compacted clay soils used as landfill liners for an acidic waste. Waste Manag 33(1):60–66. https://doi.org/10.1016/j.wasman.2012.08.012

Hudson-Edwards KA, Schell C, Macklin MG (1999) Mineralogy and geochemistry of alluvium contaminated by metal mining in the Rio Tinto Area, Southwest Spain. Appl Geochem 14(8):1015–1030. https://doi.org/10.1016/S0883-2927(99)00008-6

Hueckel T, Kaczmarek M, Caramuscio P (1997) Theoretical assessment of fabric and permeability changes in clays affected by organic contaminants. Can Geotech J 34(4):588–603. https://doi.org/10.1139/t97-013

Karathanasis AD, Hajek BF (1982) Revised methods for rapid quantitative determination of minerals in soil clays. Soil Sci Soc Am J 46(2):419–425

Kauffaman AJ, Dilling D (1950) Differential thermal curves of certain hydrous and anhydrous minerals, with a description of the apparatus used. Econ Geol 45:222–244

Knauss KG, Wolery TJ (1988) The dissolution kinetics of quartz as a function of pH aud time at 70 ° C. Geochim Cosmochim Acta 52:43–53. https://doi.org/10.1144/GSL.SP.2004.233.01.08

Knop A, VanGulck J, Heineck KS, Consoli NC (2008) Compacted artificially cemented soil-acid leachate contaminant interactions: breakthrough curves and transport parameters. J Hazard Mater 155(1–2):269–276. https://doi.org/10.1016/j.jhazmat.2007.11.056

Košek F, Culka A, Žáček V, Laufek F, Škoda R, Jehlička J (2018) Native Alunogen: a Raman spectroscopic study of a well-described specimen. J Mol Struct 1157:191–200. https://doi.org/10.1016/j.molstruc.2017.12.021

Li J s, Xue Q, Wang P, Liu L (2013) Influence of leachate pollution on mechanical properties of compacted clay: a case study on behaviors and mechanisms. Eng Geol 167:128–133. https://doi.org/10.1016/j.enggeo.2013.10.013

Liu Y, Gates WP, Bouazza A (2013) Acid induced degradation of the bentonite component used in geosynthetic clay liners. Geotext Geomembr 36:71–80. https://doi.org/10.1016/j.geotexmem.2012.10.011

Liu Y, Bouazza A, Gates WP, Rowe RK (2015) Hydraulic performance of geosynthetic clay liners to sulfuric acid solutions. Geotext Geomembr 43(1):14–23. https://doi.org/10.1016/j.geotexmem.2014.11.004

MacCarthy J, Nosrati A, Skinner W, Addai-Mensah J (2014) Dissolution and rheological behaviour of hematite and quartz particles in aqueous media at pH 1. Chem Eng Res Des 92(11):2509–2522. https://doi.org/10.1016/j.cherd.2014.02.020

Miguel MG, Barreto RP, Pereira SY (2017) Study of a tropical soil in order to use it to retain aluminum, iron, manganese and fluoride from acid mine drainage. J Environ Manag 204(4):563–570. https://doi.org/10.1016/j.jenvman.2017.09.024

Mitchell JK, Soga K (2005) Fundamentals of soil behavior. 3. ed. John Willey & Sons, New York, 560 p

Morandini TLC, Leite A d L (2015) Characterization and hydraulic conductivity of tropical soils and bentonite mixtures for CCL purposes. Eng Geol 196:251–267. https://doi.org/10.1016/j.enggeo.2015.07.011

Morse JW, Arvidson RS (2002) The dissolution kinetics of major sedimentary carbonate minerals. Earth Sci Rev 58:51–84. https://doi.org/10.1016/S0012-8252(01)00083-6

Nangia S, Garrison BJ (2010) Ab initio study of dissolution and precipitation reactions from the edge, kink, and terrace sites of quartz as a function of pH. Mol Phys 107:831–843. https://doi.org/10.1080/00268970802665621

Rose NM (1991) Dissolution rates of prehnite, epidote, and albite. Geochim Cosmochim Acta 55(11):3273–3286. https://doi.org/10.1016/0016-7037(91)90488-Q

Santos PS (1989) Ciência e Tecnologia de Argilas. Edgard Blücher Ltda, São Paulo

Sjoberg EL, Rickard DT (1984) Calcite dissolution kinetics: surface speciation and the origin of the variable pH dependence. Chem Geol 42:119–136

Streck EV, Kampf N, Dalmolin RSD, Klamt E, Nascimento PC, Giasson E, Pinto LFS (2008) Solos do Rio Grande do Sul. EMATER/RS, Porto Alegre

Šucha V, Dubiková M, Cambier P, Elsass F, Pernes M (2002) Effect of acid mine drainage on the mineralogy of a Dystric Cambisol. Geoderma 110(3–4):151–167. https://doi.org/10.1016/S0016-7061(02)00225-2

Tonnesen DA, Bertolino LC, Luz AC, Silvia FT, Timóteo DMO (2012) Caracterização Mineralógica E Beneficiamento Das Bentonitas Da Região De Cubati E Pedra Lavrada-Pb. Holos, 1: 2–14. https://doi.org/10.15628/holos.2012.821

USEPA (1996) Acid digestion of sediments, sludges, and soils - method 3050B. USEPA, Washington, USA

Verástegui-Flores RD, Di Emidio G (2014) Impact of sulfate attack on mechanical properties and hydraulic conductivity of a cement-admixed clay. Appl Clay Sci 101:490–496. https://doi.org/10.1016/j.clay.2014.09.012

Wang S, Zhu W, Fei K, Xu C, Zhang N (2018) Study on non-Darcian flow sand-clay mixtures. Appl Clay Sci 151:102–108. https://doi.org/10.1016/j.clay.2017.10.028